JOURNAL OF GEOPHYSICAL RESEARCH, VOL. 85, NO. A3, PAGES 1171-1178, MARCH 1, 1980

Nonlinear Standing Alfvén Wave Current System at Io: Theory

F. M. NEUBAUER

Institut fuer Geophysik, Technische Universität Braunschweig, 3300 Braunschweig, Federal Republic of Germany

We present a nonlinear analytical model of the Alfvén current tubes continuing the currents through Io (or rather its ionosphere) generated by the unipolar inductor effect due to Io's motion relative to the magnetospheric plasma. We thereby extend the linear work by Drell et al. (1965) to the fully nonlinear, sub-Alfvénic situation also including flow which is not perpendicular to the background magnetic field. The following principal results have been obtained: (1) The portion of the currents feeding Io is aligned with the Alfvén characteristics at an angle $\theta_A = \tan^{-1} M_A$ to the magnetic field for the special case of perpendicular flow where M_A is the Alfvén Mach number. (2) The Alfvén tubes act like an external conductance $\sum_A = 1/(\mu_0 V_A(1 + M_A^2 + 2M_A \sin\theta)^{1/2})$ where V_A is the Alfvén speed and θ the angular deviation from perpendicular flow towards the direction of Alfvén wave propagation. Hence the Jovian ionospheric conductivity is not necessary for current closure. (3) In addition, the Alfvén tubes may be reflected from either the torus boundary or the Jovian ionosphere. The efficiency of the resulting interaction with these boundaries varies with Io position. The interaction is particularly strong at extreme magnetic latitudes, thereby suggesting a mechanism for the Io control of decametric emissions. (4) The reflected Alfvén waves may heat both the torus plasma and the Jovian ionosphere as well as produce increased diffusion of high-energy particles in the torus. (5) From the point of view of the electrodynamic interaction, Io is unique among the Jovian satellites for several reasons: these include its ionosphere arising from ionized volcanic gases, a high external Alfvénic conductance $\sum_A$, and a high corotational voltage in addition to the interaction phenomenon with a boundary. (6) We find that Amalthea is probably strongly coupled to Jupiter's ionosphere while the outer Galilean satellites may occasionally experience super-Alfvénic conditions.

INTRODUCTION

The recent observations of strong electric currents associated with the Jovian satellite Io by the magnetometer experiment onboard of Voyager 1 [*Ness et al.*, 1979] have confirmed the theoretical prediction of a system of currents set up by the electric field due to Io's motion relative to the corotating magnetospheric plasma first proposed by *Piddington* [1967]; see also *Piddington and Drake* [1968]. In the picture used in most models the current system consists of field-aligned currents toward the inner face of Io as seen from Jupiter, currents through Io's interior and/or ionosphere, field-aligned currents away from Io's outer face toward the Jovian ionosphere, and final closure currents in the northern and southern Jovian dynamo region [*Goldreich and Lynden-Bell*, 1969; *Gurnett*, 1972; *Shawhan et al.*, 1975; *Dessler and Hill*, 1979]. As a first approximation the Voyager 1 magnetic field observations have been fitted by the field of a two-dimensional dipole source which can be considered as the far field of a distribution of currents approximately parallel and antiparallel to the global Jovian background magnetic field at the position of Io with net current zero. The two-dimensional dipole moment determined in this way is a vector perpendicular to the average background field which is given by

$$\mathbf{m} = \int (\mathbf{x} - \mathbf{x}_D) \times \mathbf{j}\, dS \qquad (1)$$

where $\mathbf{j}$ is the current density, $\mathbf{x}$ the position vector and $\mathbf{x}_D$ the location of the dipole in the plane perpendicular to $\mathbf{j}$ with area elements dS. It is clear from (1) that determination of the total current requires further modeling, since it is $\mathbf{m}$ which directly follows from the observations if we accept the assumption that Voyager 1 has observed the far or at most intermediate range magnetic perturbation field of a current distribution described by a bundle of currents limited in cross-sectional area. Increasing the average distance between the antiparallel parts of the current distribution implies decreasing the total currents to be consistent with the determination of $\mathbf{m}$. However, in spite of this model dependence it is difficult to escape the conclusion that the magnetic field in the vicinity of Io is strongly perturbed by the presence of the satellite associated current system. Also we wish to point out that the observations do not rule out the possibility of internal magnetic fields influencing the current system in the vicinity of Io [*Neubauer*, 1978; *Kivelson et al.*, 1979].

In the model using field-aligned currents outside of Io the plasma inertia is neglected. Physically, the short-circuiting of the corotational electric fields by the conductance associated with Io or its ionosphere leads to electric field variations which imply velocity variations and therefore acceleration or deceleration of the plasma. These acceleration terms must be balanced by $\mathbf{j} \times \mathbf{B}$ forces. Consequently, the perpendicular component of the currents increases in relative importance as the mass density increases. The unipolar inductor model including plasma inertia has been treated theoretically by *Drell et al.* [1965] in the simple approximation of linear perturbations only. It has been shown by these authors that the current is not field aligned and is associated with Alfvén waves—called Alfvén 'wings'—standing in the satellite frame of reference. The significance of these inertial effects can be expressed by the Alfvén Mach number

$$M_A = u_0/V_A \qquad (2)$$

with u_0 the relative speed between Io and the magnetospheric flow and V_A the Alfvén speed. Figure 1 sketches the basic configuration obtained by *Drell et al.* [1965]. Since the current is guided by the wings or Alfvén current region, the spatial separation between the current stream lines and magnetic field lines may be appreciable even for small values of M_A if followed down to Jupiter's ionosphere. Some different aspects of Alfvén wave generation by a conducting Io have been treated by *Goertz* [1973] and *Goertz and Deift* [1973]. In the terrestrial magnetosphere, *Maltsev et al.* [1977] have applied the more accurate concept of Alfvénic current systems to 'field-aligned'

Paper number 9A1540.
0148-0227/80/009A-1540$01.00

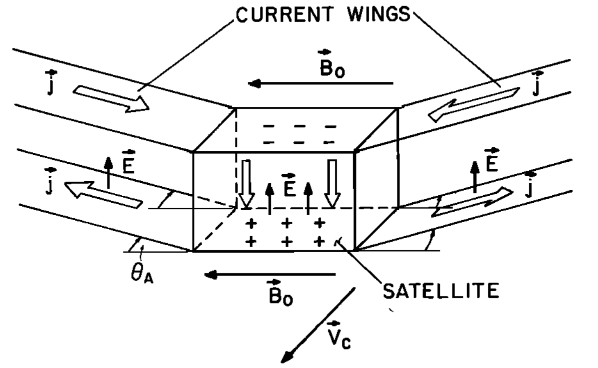

Fig. 1. Three-dimensional sketch of 'Alfvén wings' generated by an ideal conductor in a collisionless plasma [after *Drell et al.*, 1965]. $\mathbf{V}_c$ is the satellite speed with respect to the plasma. The Alfvén wings are bent away from $\mathbf{B}_0$ by θ_A given by (4).

currents of auroral arcs. This work has been amplified by *Mallinckrodt and Carlson* [1978].

We can use the preliminary plasma and radio astronomy results at the time of the Voyager 1 encounter [*Bridge et al.*, 1979; *Warwick et al.*, 1979] to obtain an upper limit to the Alfvén speed or lower limit to the Alfvén Mach number. Figure 4 of *Warwick et al.* [1979] yields a density of $n \sim 1500$ cm^{-3}, which, assuming that the ion species is protons, yields $V_A \sim$ 1070 km/s and $M_A \sim 5.3 \times 10^{-2}$. Massive ions like S^{++} will further increase the Alfvén Mach number. Using the upper density limits obtained by *Broadfoot et al.* [1979] for a uniform density model of the torus we obtain $M_A \leq 0.18$. Conversely, we show below how the magnetic field data can be used to obtain an independent estimate of M_A, and therefore the mass density ρ.

The brief discussion above indicates that a self-consistent model of the interaction between Io's ionosphere and/or interior and Jupiter's magnetosphere must include the appreciable distortions of the magnetic field in a nonlinear model. In this paper we present a theoretical treatment of the Alfvén wings or, more generally, Alfvén current tubes in the framework of nonlinear magnetohydrodynamics. The motivation is twofold. First, we wish to lay the foundation for a proper local physical modeling of the Voyager observations which allows, for example, a reasonably accurate tracing of high-energy charged particle trajectories to Io's close vicinity. A detailed modeling of the magnetic field observations of Voyager 1 [see *Ness et al.*, 1979] is done in a paper by M. H. Acuna et al. (unpublished manuscript, 1979). Second, we thereby self-consistently treat one aspect of the complete Io problem in the vicinity of the satellite including important nonlinearities. We also discuss the interaction of the Alfvén tubes with the magnetosphere and with the Io associated plasma torus in particular. Finally, we briefly apply our theoretical results to the five innermost satellites of Jupiter.

ANALYSIS

Figure 2 shows a schematic sketch of the interaction geometry. We also take into account a deviation θ of the speed $\mathbf{V}_0$ from being perpendicular to the magnetic field $\mathbf{B}_0$ as indicated in Figure 3. We assume sub-Alfvénic flow, i.e., $M_A < 1$. Consequently, no bow shock can form. Because of Io's volcanic activity, a highly dynamical thin neutral atmosphere and ionosphere are expected which probably form a tail downstream, similar to the basic idea of *Cloutier et al.* [1978]. Because $M_A <$ 1, fast MHD disturbances can propagate in all directions, whereas the propagation of Alfvénic and slow MHD disturbances is restricted by the geometry of their characteristics. Figure 2 also illustrates some Alfvén and slow characteristics for small disturbances. If we further make the reasonable assumption of the magnetic field pressure exceeding the thermal plasma pressure at some distance from Io, the region of main Alfvénic disturbances is separated from the region perturbed by slow disturbances. The fast MHD disturbances generated by Io propagate away from the satellite in an approximately isotropic manner thus decreasing in amplitude. Therefore the Alfvénic perturbations will become quite pure unless local generation of slow or fast disturbances is important. We wish to point out, however, that the fast mode and also slow mode disturbances will play an important role in closing part of the currents flowing inside Io or its ionosphere as M_A increases toward one (a more accurate condition is obtained by taking into account the plasma pressure) when a fast shock forms. Note that in the paper by *Drell et al.* [1965] no such currents are included because of the assumption of very low M_A which may not necessarily be adequate for the Galilean satellites.

After these general preparations we now turn to the treatment of the nonlinear Alfvén disturbances. The theoretical treatment of Io's vicinity is deferred to a later paper. We assume uniformity of the magnetospheric magnetic field and plasma in the region of interest. Our analysis will be performed in the rest frame of Io. The Alfvén characteristics $C_A^{\pm}$ are given by lines along the total group velocities

$$\mathbf{V}_A^{\pm} = \mathbf{V} \pm \frac{\mathbf{B}}{(\mu_0 \rho)^{1/2}} \tag{3}$$

where $\mathbf{V}$ is the plasma speed in one-fluid MHD, ρ the mass density, and $\mathbf{B}$ the magnetic field vector. The plus sign and minus sign denote propagation toward the southern hemisphere and northern hemisphere of Jupiter, respectively. The linear solutions [e.g., *Drell et al.*, 1965] imply constancy of all perturbed quantities along $\mathbf{V}_A^{\pm}$. Here $\mathbf{V}_A^{+}$ is given by the constant background properties $\mathbf{V}_0$, $\mathbf{B}_0$, and ρ. Let us now look for a nonlinear standing Alfvén wave solution which is independent of the coordinate along a fixed direction. Since this direction must also apply for the outer part of the Alfvén perturbation region with small (i.e., linear) perturbations, this

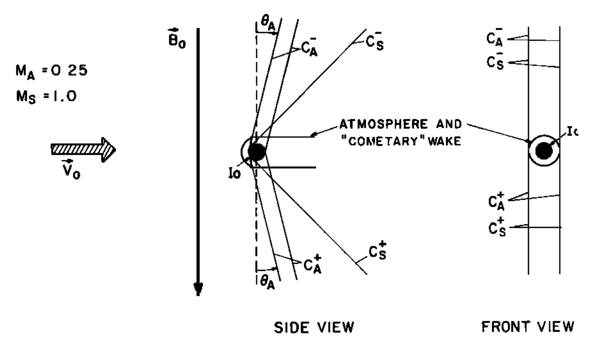

Fig. 2. Examples of linear Alfvén and slow wave characteristics for $M_A = 0.25$ and sonic Mach number $M_s = u_0/a_0 = 1$ with the speed of sound a_0. Front view and side view refer to an observer moving with the plasma approaching Io. Alfvén characteristics $C_A^{\pm}$ delineate range of influence due to the Alfvén mode. Slow characteristics $C_S^{\pm}$ delineate range of influence due to slow mode propagation. Fast mode waves can propagate in all directions. Strong Alfvénic disturbances are expected to issue from Io and its vicinity along the appropriate tube of Alfvén characteristics. Slow disturbances are issuing along their characteristics from Io's vicinity and the wake region. Both do not propagate perpendicular to $\mathbf{B}_0$ as shown in the front view.

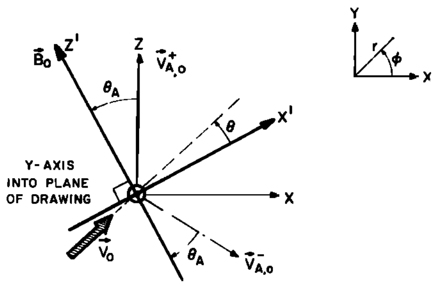

Fig. 3. Geometrical relationships and coordinate systems used in this work. Note that θ is positive if $\mathbf{V}_0$ and $\mathbf{V}_A^+$ are on the same side of the x' axis and vice versa.

direction must be identical to the direction of $\mathbf{V}_A^{\pm}$ in the unperturbed region, i.e.,

$$\mathbf{V}_{A,0}^{\pm} = \mathbf{V}_0 \pm \frac{\mathbf{B}_0}{(\mu_0 \rho)^{1/2}}$$

We shall consider southward propagation of Alfvén waves for definiteness without loss of generality. For the analysis we shall choose the coordinate system shown in Figure 3 with z along $\mathbf{V}_{A,0}^+$ and x in the plane of z and corotational flow. The angle θ_A between $\mathbf{B}_0$ and $\mathbf{V}_{A,0}^+$ is given by

$$\sin \theta_A = \frac{M_A \cos \theta}{(1 + M_A^2 + 2M_A \sin \theta)^{1/2}} \qquad (4)$$

Assuming ρ, the pressure p, $|\mathbf{B}|$, and $\mathbf{V}_A^+$ to be constant with

$$\mathbf{V}_A^+ = V_{A,0}^+ = \mathbf{V} + \frac{\mathbf{B}}{(\mu_0 \rho)^{1/2}} \qquad (5)$$

we automatically satisfy the equation of mass conservation and the equation of motion

$$\rho(\text{curl } \mathbf{V} \times \mathbf{V} + 1/2 \nabla \mathbf{V}^2) = -\nabla p + \mathbf{j} \times \mathbf{B} \qquad (6)$$

as well as the frozen-in field condition $\mathbf{E} + \mathbf{V} \times \mathbf{B} = 0$ which implies

$$\text{curl } (\mathbf{V} \times \mathbf{B}) = -\mathbf{B} \text{ div } \mathbf{V} + (\mathbf{B} \cdot \nabla) \mathbf{V} - (\mathbf{V} \cdot \nabla) \mathbf{B} = 0 \qquad (7)$$

This is easily shown by replacing $\mathbf{B}$ in (6) and (7) using (5) and Ampere's law. The equation div $\mathbf{B} = 0$, which is needed for the derivation of (7), is fulfilled because of (5) and the constancy of ρ. Stationarity implies

$$\mathbf{E} = -\vec{\nabla}\psi = (E_x, E_y, 0) \qquad (8)$$

where ψ is the scalar electric potential depending on the coordinates x and y only. An important relation for the component of the current density $\mathbf{j}$ in the z direction can be obtained using (5) again:

$$\text{div } \mathbf{E} = -\mathbf{B} \cdot \text{curl } \mathbf{V} + \mathbf{V} \cdot \text{curl } \mathbf{B} = \mathbf{V}_A^+ \cdot \mathbf{j}\mu_0$$

And finally,

$$j_z = \Sigma_A \text{ div } \mathbf{E} = -\Sigma_A \nabla^2 \psi \qquad (9)$$

with

$$\Sigma_A = \frac{1}{\mu_0 V_A (1 + M_A^2 + 2M_A \sin \theta)^{1/2}} \qquad (10)$$

Σ_A has the dimension of a conductance.

We may consider any current circuit in Io's vicinity to be 'closed' by a conductance Σ_A due to Alfvén waves. For example, an Alfvén speed of 1000 km/s together with $M_A \ll 1$ leads to $\Sigma_A = 0.8\ \Omega^{-1}$. We have used quotes to indicate that in the absence of any boundary which might reflect the Alfvén wave the currents along ($+z$) or ($-z$) extend to infinity where they may be considered to close or to be fed by sources and sinks. Thus the unipolar inductor also works without current closure in the Jovian ionosphere. Real current closure will occur by losses during reflection at the Jovian ionospheric boundary, due to absorption in the magnetosphere, etc. Equations (9) and (1) can be used to derive a general expression for the two-dimensional dipole moment in the plane x, y. The part of the current density vector $\mathbf{j}$ in the z direction is given by $j_z \cdot \mathbf{z}_u$, where $\mathbf{z}_u$ is the unit vector in the direction of positive z. In the equation $\mathbf{m} = (\Sigma_A \iint (\mathbf{x} - \mathbf{x}_D) \text{ div } \mathbf{E}\, dS) \times \mathbf{z}_u$ with $dS = dxdy$ the electric field $\mathbf{E}$ can be replaced by the constant perturbation electric field $\mathbf{E}_p = \mathbf{E} - \mathbf{E}_0$, where the background electric field $\mathbf{E}_0$ is given by

$$\mathbf{E}_0 = -\mathbf{V}_0 \times \mathbf{B}_0 = (0, u_0 B_0 \cos \theta, 0) \qquad (11)$$

Using the summation convention, the expression $(\mathbf{x} - \mathbf{x}_D)$ div $\mathbf{E}_p$ can be written as

$$(x_i - x_{D,i}) \frac{\partial E_{p,k}}{\partial x_k} = \frac{\partial}{\partial x_k} [(x_i - x_{D,i}) E_{p,k}] - \delta_{i,k} E_{p,k}$$

where $\delta_{i,k}$ is the Kronecker delta. If we assume that net current along z, i.e., $\int j_z dS$ to be zero, the first term on the right-hand side contributes $\mathbf{m}/2$ to the integral for $\mathbf{m}$ upon application of Gauss's theorem, and we obtain

$$\mathbf{m} = 2\Sigma_A\, \mathbf{z}_u \times \int \mathbf{E}_p\, dS \qquad (12)$$

If Σ_a is known, an observed magnetic moment yields therefore the integrated perturbation electric field.

The current components perpendicular to $\mathbf{V}_A^+$ are given by

$$\mathbf{j}_\perp = (j_x, j_y, 0) = \frac{1}{\mu_0} \nabla B_z \times \mathbf{z}_u = -\frac{B}{B_z} \nabla B \times \mathbf{z}_u \qquad (13)$$

The dependence of $\mathbf{j}$ on x and y only implies that $j_z \cdot \mathbf{z}_u$ and $\mathbf{j}_\perp$ have divergence zero separately. Therefore the current field $\mathbf{j}_\perp$ forms closed loops in the x, y plane. These currents can geometrically connect to Io only in its vicinity. On the other hand, the currents $j_z \cdot \mathbf{z}_u$ then constitute the currents feeding the complex three-dimensional current system in Io's immediate vicinity.

A general solution of the type discussed here can be constructed in the following way: Specification of $j_z(x, y)$, using (8) and (9) and the additional condition $\mathbf{E} \rightarrow \mathbf{E}_0$ for $r = (x^2 + y^2)^{1/2} \rightarrow \infty$, allows the complete determination of ψ. From $E = -\mathbf{V} \times \mathbf{B}$ and (5) we obtain

$$\mathbf{B}_\perp = (B_x, B_y, 0) = (\mathbf{z} \times \mathbf{E})\mu_0 \Sigma_A \qquad (14)$$

B_z is obtained from

$$B_z = \pm(B_0^2 - B_\perp^2)^{1/2} \qquad (15)$$

and the speeds $\mathbf{V}$ are obtained from (5). If the currents parallel to $\mathbf{z}_u$ (or $\mathbf{V}_A^+$) are restricted to be inside a cylinder with radius R_c, the potential outside is simply given by the general Laplacian solution

$$\psi = -E_0 y + \sum_{n=1}^{\infty} (A_n \cos n\phi + B_n \sin n\phi)(R_c/r)^n + A_0 \log (R_c/r) \qquad (16)$$

where ϕ is the position angle in the x, y plane and $r = (x^2 + y^2)^{1/2}$. If the net current $\iint j_z\, dx\, dy = 0$, we can omit the term involving A_0. Equation (14) provides a simple relation of the electric field expansion to the magnetic field expansion outside R_c.

For use in the analysis of observational data it is reasonable to finally consider the magnetic field perturbation vectors defined by

$$\mathbf{B}_p = \mathbf{B} - \mathbf{B}_0 \tag{17}$$

in the linear case, i.e., at some distance from the Alfvén tube. It is well known that in the linear case, $\mathbf{B}_p$ is perpendicular to $\mathbf{B}_0$ for an Alfvén wave. In the primed coordinate system, which is also shown in Figure 3, we have

$$\begin{aligned} B_{p,z'} &= 0 \\ B_{p,y'} &= B_{p,y} = E_x \mu_0 \Sigma_A \\ B_{p,x'} &= B_{p,x}(1 + \tan^2 \theta_A)^{1/2} \\ &= -(E_y - u_0 B_0 \cos \theta)\mu_0 \Sigma_A (1 + \tan^2 \theta_A)^{1/2} \end{aligned} \tag{18}$$

after linearization. It is interesting to compare these perturbation fields with the external magnetic field of currents flowing solely parallel to $\mathbf{B}_0$ used in the preliminary analysis of *Ness et al.* [1979]. The representations differ by the factor $(1 + \tan^2 \theta_A)^{1/2}$ in the expression for $B_{p,x'}$. Equation (18) also shows that the normal to the plane of the perturbation field x', y' differs by θ_A in direction from those currents feeding the current system in Io's vicinity. In the nonlinear regime close to the Alfvén tube the perturbation vectors do not necessarily lie in a plane.

We note that instead of the elementary derivation in this section we might have used a mathematical shortcut using the theory of simple waves where $\mathbf{V}_A$ corresponds to a Riemann invariant [e.g., *Jeffrey and Taniuti*, 1964].

The above developments open interesting possibilities for the evaluation of magnetic field observations made close to the Alfvén tube. Since the currents along $\mathbf{V}_A^+$ or $\mathbf{V}_A^-$ must be closed in the vicinity of Io, this condition together with the determination of the location of the Alfvén tube relative to the spacecraft trajectory can be used to determine the orientation of the Alfvén characteristics. Since the angle between $\mathbf{V}_A^\pm$ and $\mathbf{B}_0$ involves the corotational speed and plasma mass density in addition to the magnetic field vector according to (4), it opens up the possibility of determining the plasma mass density from magnetic field data alone. This possibility is certainly interesting for both the Voyager 1 and future Galileo observations.

Two-Dimensional Electric Dipole

As an example, we consider the important case of a two-dimensional electric dipole field with $A_n = 0$ and $B_n \neq 0$ for $n \neq 1$ only. We assume j_z to be distributed over a cylinder $r = R_{Io}$ according to a sin ϕ law, where the angle ϕ has been defined in Figure 3. This model seems to be a reasonable first approximation to the Io Alfvén tube before an accurate modeling of the vicinity of Io. Inside the cylinder the electric field $\mathbf{E}_i$ is constant in this case. Using $E_i < E_0$, we obtain

$$\psi = -E_i r \sin \phi \qquad r \leq R_{Io}$$

and

$$\psi = -E_0 r \sin \phi + (E_0 - E_i) R_{Io} (R_{io}/r) \sin \phi \qquad r > R_{Io} \tag{19}$$

For $\mathbf{B}$ we obtain

$$B_x = -E_i \mu_0 \Sigma_A \qquad r < R_{Io} \tag{20}$$

$$B_y = 0 \qquad r < R_{Io}$$

$$B_x = \left(-E_0 + R_{Io}^2 (E_0 - E_i) \frac{x^2 - y^2}{r^4}\right) \mu_0 \Sigma_A \qquad r \geq R_{Io} \tag{21a}$$

$$B_y = R_{Io}^2 (E_0 - E_i) \frac{2xy}{r^4} \mu_0 \Sigma_A \qquad r \geq R_{Io} \tag{21b}$$

with B_z given by (15). The two-dimensional dipole moment in the x, y plane is given by

$$m_x = 2\pi R_{Io}^2 (E_0 - E_i) \Sigma_A \qquad m_y = 0 \tag{22}$$

which is also a special case of (12). If the electric field inside the cylinder is short-circuited completely by the conductance of the Ionian current path, i.e., $E_i = 0$, we obtain the maximum magnetic moment of

$$m_x = \frac{2\pi R_{Io}^2 B_0 \cos \theta\, M_A}{\mu_0 (1 + M_A^2 + 2M_A \sin \theta)^{1/2}}.$$

Assuming the maximum number for $M_A = 0.18$, $R_{Io} = 1820$ km, and $B_0 = 1900$ nT, we obtain $m_x = 5.6 \times 10^9$ A km, somewhat less than the lower limit obtained in the regression analysis of *Ness et al.* [1979]. This suggests that even for a complete short-circuiting the current-carrying cylinder must have a greater diameter than R_{Io} or for incomplete short-circuiting the diameter must be even greater. The latter interpretation would imply that Joule heating of Io or its ionosphere is small in comparison with the energy radiated away in Alfvén waves and possibly dissipated in the 'external load.' Finally, the observational evidence for the existence of a neutral atmosphere consisting mainly of SO_2 [*Pearl et al.*, 1979; *Kumar*, 1979] suggests that the resulting ionosphere could provide a conducting region with an effective radius greater than R_{Io} to close the Alfvénic currents. Here, j_z is given as a surface current density $j_{z,s}$ on $r = R_{Io}$,

$$j_{z,s} = 2\frac{B_0}{\mu_0}\left(1 - \frac{E_i}{E_0}\right) \sin \phi \sin \theta_A \tag{23}$$

which integrates to a total current of

$$I = 4(E_0 - E_i) R_{Io} \Sigma_A \tag{24}$$

in each direction. This has an interesting consequence. Even for zero internal resistance of the unipolar generator, i.e., $E_i = 0$, the total current is limited to a maximum value $I_{max} = 4E_0 R_{Io} \Sigma_A$ due to the Alfvén conductance in (10).

There is also a perpendicular surface current component $j_{\phi,s}$ in the cylinder $r = R_{Io}$ given by

$$j_{\phi,s} = -\frac{B_0}{\mu_0} \cdot \cos \theta_A \{[1 - \tan^2 \theta_A (\eta - 1)(\eta - 1 + 2\cos 2\phi)]^{1/2} - [1 - \tan^2 \theta_A (\eta^2 - 1)]^{1/2}\} \tag{25}$$

where we have used $\eta = E_i/E_0$. It is connected to volume currents which finally decrease as r^{-3} at large distances from the cylinder according to (13). From the discussion following (13) the total surface current vectors on the cylinder are neither field-aligned nor divergenceless.

The velocity is given by

$$\mathbf{V} = u_0[\cos(\theta_A + \theta), 0, \sin(\theta_A + \theta)] - \frac{\mathbf{B} - \mathbf{B}_0}{(\mu_0 \rho)^{1/2}} \tag{26}$$

Equation (21) can also be viewed as describing a homogeneous field plus the magnetic field of a two-dimensional magnetic dipole due to the current distribution $j_z(x, y)$ along the characteristic C_A^+ alone. For such a magnetic dipole alone, B_z would be constant. However, in the Alfvén tube, $|\mathbf{B}| = B_0$ is forced to be constant by the currents $\mathbf{j}_\perp$.

The distortion of the magnetic field lines is interesting for several reasons. These include high-frequency wave tracing computations and the trajectories of energetic particles. Figure 4 shows an extreme case of the field lines passing through the Alfvén tube at $y = 0$ for $E_i = 0.0909E_0$ and $M_A = 0.5$. Note that field lines outside the midplane $y = 0$ have a bulge away from the midplane as they pass by or through the current-carrying cylinder.

We may finally estimate the Joule dissipation in Io by assuming closure of the current I by currents parallel to $\mathbf{E}_i$ inside the cylinder and at the end of it. This neglects the correct conductivity distribution in and around Io and magnetic field distortion, to name the most important items. Using (23), we obtain

$$P = 2 \times \left(\frac{\pi}{4}\right) \times (2R_{Io}E_i) \times \left(4\frac{B_0}{\mu_0}R_{Io}\left(1 - \frac{E_i}{E_0}\right)\sin\theta_A\right)$$

or, after some rearrangement using (4) and (10),

$$P = 4\pi R_{Io}^2 E_i(E_0 - E_i)\Sigma_A \tag{27}$$

The maximum Joule dissipation occurs for optimum matching of internal and external loads, implying $E_i = E_0/2$ and

$$P_{max} = \pi R_{Io}^2 E_0^2 \Sigma_A \tag{28}$$

It is interesting to note the average volume heating rate P_{max}/Volume $= \frac{3}{4} E_0^2\Sigma_A/R_{Io}$. Also the Ionian conductivity for optimum matching is of the order Σ_A/R_{Io} apart from a factor not much different from unity.

SIGNIFICANCE OF SATELLITE-INDUCED ALFVÉN WAVE SYSTEMS

In the last earlier section we presented a nonlinear solution for the standing Alfvén wave system generated by Io or any other satellite moving relative to a homogeneous magnetoplasma at sub-Alfvénic speeds. This solution may serve as the theoretical background for a local fitting to magnetic field or other observations (M. H. Acuna et al., unpublished data, 1979). In this section we shall discuss some of the interesting consequences of the system of Alfvén tubes radiated by Io and observed by the Voyager 1 magnetometer experiment [*Ness et al.*, 1979].

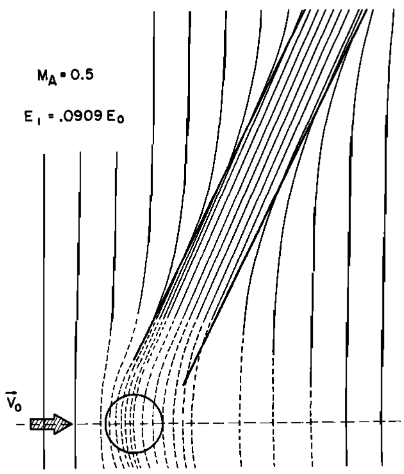

Fig. 4. Magnetic field lines in plane $y = 0$ for $M_A = 0.5$ and $E_i = 0.0909E_0$. The large value of M_A has been chosen for clarity. In the vicinity of Io the expected field line topology has been sketched, whereas solid lines are due to the theory developed in this paper. Note that for $E_i \ll E_0$ the field lines inside the cylinder are parallel to the cylinder and for the trivial case $E_i = E_0$ the field lines are straight lines everywhere.

Following the Alfvén tubes through the Jovian magnetosphere requires taking into account the inhomogeneous magnetic field and plasma distribution. This will lead to a bending of the Alfvén current tubes and other associated changes. Strong gradients in plasma mass density lead to reflection of Alfvén waves. There are at least two potential boundary regions with high-density gradients. First we may have strong reflection from the boundary of the plasma torus centered around the magnetic equator at a distance of 6 R_j [*Broadfoot et al.*, 1979; *Warwick et al.*, 1979; *Gurnett et al.*, 1979; *Bridge et al.*, 1979]. Using whistler dispersion, *Gurnett et al* [1979] have shown that the electron density decreases from up to 4000 cm^{-3} in the center of the torus to less than 20 cm^{-3} outside. Although there are physical reasons to assume a higher average ionic mass in the torus than in its surroundings, even the assumption of identical chemistry leads to an increase of at least an order of magnitude in Alfvén speed across the torus boundary at the time of the Voyager encounter. Consequently, strong reflection may occur. Second, the Jovian ionosphere is a potential reflecting boundary for the Alfvén waves due to Io. Figure 5 shows a sketch of the scenario expected for a position of Io in the center of the torus and at maximum magnetic latitude.

In the situation shown in Figure 6*a* there is no interaction between Io's immediate vicinity and any of the reflected Alfvén waves. The Alfvén tube provides the external resistance Σ_A given by (10). The interaction occurs if one of the reflected Alfvén wave tubes is able to return to Io before the satellite has moved away. If the distance from the reflecting boundary is L_R and we assume $\theta = 0$ for simplicity in Figure 3, the condition under which the interaction will occur is

$$\int_0^{L_R} \frac{ds}{V_A} < \frac{R_{Io}}{u_0} \tag{29a}$$

or

$$M_A < R_{Io}/L_R \tag{29b}$$

for a uniform propagation path. It is most difficult to fulfill this condition if Io is in the magnetic equatorial plane. Assuming a constant Alfvén speed in the torus of diameter 2 R_J, the Alfvén Mach number must be less than R_{Io}/R_J to have a strong interaction, i.e., $M_A < 0.025$ or the mass density $\rho \leq 350 m_p/\text{cm}^3$ where m_p is a proton mass. The plasma density during the encounter of Voyager 1 was too large for the interaction to occur. However, depending on the precise density distribution, conditions under which the interaction will occur are easiest to fulfill if Io is at maximum or minimum magnetic latitude, i.e., with the magnetic dipole of Jupiter tipping toward or away from Io. In this situation, Io may even be outside the torus if we invoke some azimuthal variations in torus diameter. If instead of this somewhat extreme possibility the more conservative assumption is made that the torus is formed by ions originating from Io and bouncing around the magnetic equator in an unimpeded way, Io would be located in the region of strong density decrease near the torus bound-

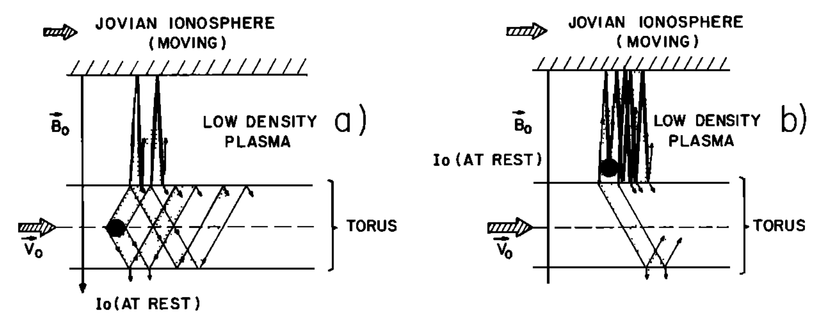

Fig. 5. Sketch of Alfvén current tube system associated with Io. Reflections occur at torus boundaries and Jovian ionosphere. Propagation directions are indicated. Regions of space affected by Alfvén current tubes are shown dotted. Continuation of the wave regions shown will finally lead to an almost complete filling with Alfvén waves to the right of the leftmost Alfvén tube. (*a*) Io in magnetic equatorial plane. No interaction due to Alfvén waves reflected back to Io. Only Rhombus immediately following Io not reached by Alfvén waves. (*b*) Io at maximum magnetic latitude outside torus. Strong interaction with the torus boundary and Jovian ionosphere due to reflected Alfvén waves.

ary at maximum magnetic latitude. In any case at this time the interaction between Io and the Jovian ionosphere will be most efficient via the Alfvén wave reflected from the Jovian ionosphere. In the limit that inequality (29) is fulfilled strongly for the Jovian ionosphere reflection, we may have the limit of an Alfvénic current system proposed by *Piddington* [1967], i.e., the currents are almost field aligned in the magnetosphere and are closed through the Jovian dynamo region. From the discussion above, it appears that the coupling between Io and the Jovian ionosphere is strongest for maximum magnetic latitude excursions. We propose that in addition to beaming, this is the physical reason for the Io control of decametric emissions which is maximum at maximum northern latitude of Io [see *Dulk*, 1965]. To explain the absence of Io-controlled emissions at maximum southern magnetic latitude, we observe that the magnetic field magnitude in the vicinity of Jupiter is much greater in the northern polar region than in the southern polar region [*Acuna and Ness*, 1976]. This leads to a higher Alfvén speed and therefore to a stronger coupling via northerly Alfvén current tubes in the sense of (29*a*) unless the magnetic field magnitude enhancement is compensated by a density enhancement.

Strong reflection of Io's Alfvén tubes from the inner torus boundary will lead to a sequence of standing Alfvén waves reflected back and forth between the boundaries. These reflected Alfvén tubes may produce increased diffusion of radia-

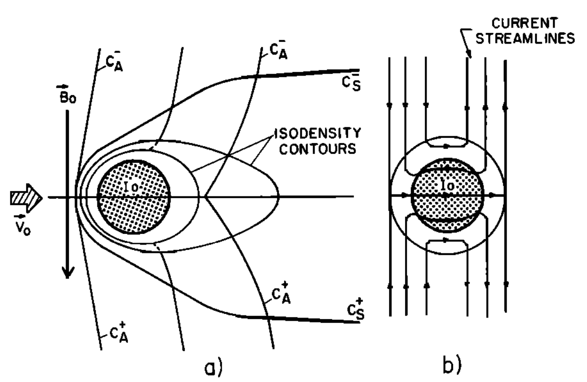

Fig. 6. Sketch illustrating modification of slow and Alfvénic characteristics due to interaction leading to enhanced densities above poles due to 'polar wind' outflow from Ionian ionosphere. (*a*) View in *x*, *z* plane. Note bending of characteristics $C_A^\pm$ due to enhanced densities and of $C_S^\pm$ due to decreased sonic Mach number in short-circuited low-velocity region. (*b*) Sketch of current flow seen from front side.

tion belt particles via their associated electric and magnetic field perturbations. The mapping of electric fields via the Alfvén characteristics can be pictured as a sequence of images of Io, e.g., in the Jovian magnetic equatorial plane.

The reflecting waves in Figure 5 must finally lose their energy by dissipation either by Joule heating in the Jovian dynamo region or by damping and associated particle heating of the Alfvén waves proper in the torus or other wave types generated, e.g., by reflection at the torus boundary. Waves reflected back to Io will lose part of their energy in the dynamo region of Io's ionosphere. The possible return of reflected waves and interaction with the Jovian ionosphere may even lead to power dissipation in Io or its ionosphere which exceed P_{max} in (28) under favorable conditions. The relative importance of all these processes can only be assessed after proper modeling.

Several complications will make the picture described even more difficult. First, reflection of the Alfvén waves will also produce other wave modes like fast waves. Second, with a cyclotron frequency of an S^{++} ion in a 1900-nT magnetic field of $f_c(S^{++}) = 1.8$ Hz, finite ion gyroradius effects cannot be neglected for length scales of the order of $u_0\ [2\pi f_c(S^{++})]^{-1} = 5.1$ km, which should be compared with an atmospheric scale height of 7.1 km for SO_2 at 100 K on Io. Current filaments of these scales will propagate in a much more complex manner than the 'simple' Alfvén wave picture suggests. In fact, each of the gas volcanoes may contribute its pair of Alfvénic current filaments with diameters given by the associated gas clouds.

Strong short-circuiting of electric fields by Io's ionosphere implies a strong reduction of plasma speeds in Io's frame, which also implies a long time for the passage of a flux tube across Io's diameter. A long time is then available for emptying the plasma of the flux tubes into Io's atmosphere, where it will lead to enhanced ionization. Conversely, Joule heating in the upper layers of Io's atmosphere-ionosphere system may lead to a polar wind flow filling flux tubes passing above and below Io with plasma up to distances determined by the characteristics $C_s^\pm$ of slow waves in a fluid picture. In a plasma with dominant magnetic field pressure the $C_s^\pm$ are along $\mathbf{V}_s^\pm = \mathbf{V} \pm (\mathbf{B}/B)a$, where a is the appropriate sound speed. The situation has been sketched in Figure 6. A net change in mass density due to the latter effects will also change the Alfvén tube as schematically indicated in Figure 6. We close the discussion with these remarks which already point to some of the interesting questions to be treated in physical models of Io's immediate vicinity.

NUMERICAL RESULTS

It is finally interesting to apply the theoretical results developed above to the Galilean satellites and Amalthea. Some simple results are shown in Table 1. The satellite speeds u_0 relative to the plasma have been obtained assuming corotation. This assumption is questionable at Callisto and sometimes even closer to Jupiter [*McNutt et al.*, 1979]. The electron densities n_e have been obtained from *Warwick et al.* [1979] at Io and from *Bridge et al.* [1979] for the outer satellites. For Amalthea we have simply assumed $n_e = 20$ cm^{-3}. We assume an average ion mass per electron of 9 proton masses m_p, which corresponds to the upper limit torus composition of *Broadfoot et al.* [1979]. Although this assumption is not consistent with the *Bridge et al.* [1979] densities which were derived assuming protons as the dominant species both the observational uncertainties and variations make this a not too unreasonable assumption. It is important to note at this point that the torus is subject to appreciable temporal variations as shown by ground-based observations [e.g., *Mekler and Eviatar,* 1978] and also a comparison of Pioneer 10 and Voyager observations [*Broadfoot et al.*, 1979]. The magnetic fields have been derived from a dipole with 3.9 G R_J^3 for the inner four satellites and from the directly measured value for Callisto [*Ness et al.*, 1979].

The Alfvén Mach number M_A, the angle θ_A ($\theta = 0$), the voltage U applied to the satellite, Alfvénic conductance Σ_A, maximum current (equation (24) for $E_t = 0$), maximum magnetic moment, and maximum power dissipation in the satellite have been included for the two-dimensional electric dipole model. The table also contains Σ_A/R, the approximate internal conductivity for best matching of internal and external loads. The entries in Table 1 following Σ_A assume simple radiation of Alfvén waves without interaction due to waves reflected back to the satellite. If an effective satellite radius greater than the geometrical radius is chosen, the maximum values of total current, magnetic moment, and power dissipation will be even greater. For example, an extensive ionosphere of Io results in a greater effective satellite radius. It is clear from the table that the uniqueness of Io results not only from volcanism finally leading to a conducting ionosphere but to at least the same extent from the low external resistance Σ_A^{-1} provided by the huge torus densities combined with a large voltage U driving the currents. In addition, the possibility of fulfilling the inequality (29) for interaction with the Jovian ionosphere or the torus boundary gives Io an advantage compared with the other Galilean satellites. Moreover, the outer satellites probably lack sufficient conductivity because of the absence of an adequate ionosphere and/or an internal conductive path. The Mach numbers suggest that sometimes a transition to super-Alfvénic flow may occur at least for Ganymede and Callisto leading to a more lunar type interaction if they possess no internal magnetic field or sufficient conductivity. The value for the maximum power dissipation inside Io or its ionosphere far exceeds the nominal power of 10^8 W required for decametric radio bursts [*R. A. Smith,* 1976]. Although an important diagnostic tool, decametric radio emissions are therefore probably unimportant for the energy balance of the overall current system.

Amalthea is probably coupled to the Jovian ionosphere most of the time according to θ_A. The maximum possible power may therefore exceed P_{max} appreciably depending on the Jovian ionospheric conductance. Since the optimum internal conductivity Σ_A/R in Table 1 already exceeds a typical silicate conductivity at the temperature of Amalthea by several orders of magnitude, the real power dissipation is determined by the satellite's conductivity leading to values even smaller than P_{max} in Table 1.

CONCLUSIONS

We have presented a fully nonlinear analytical solution for the standing Alfvén wave current system, detected by Voyager 1, feeding the current system in the immediate vicinity of Io. The latter is probably generated by the unipolar inductor effect suggested by *Piddington* [1967]. We have obtained the following main theoretical results:

1. Current flow deviates appreciably from magnetic field lines where the part of the currents connected with the generator, i.e., Io, flows along Alfvén characteristics $C_A^{\pm}$ given by $\mathbf{V}_A^{\pm} = \mathbf{V}_0 \pm \mathbf{B}_0/(\mu_0\rho)^{1/2}$. For perpendicular flow the angle θ_A between the $C_A^{\pm}$ and the magnetic field is given by $\tan\theta_A = M_A$, where M_A is the Alfvén Mach number.

2. An additional system of currents perpendicular to the characteristics $C_A^{\pm}$ is closed in loops not generally connecting to Io.

3. The nonlinear Alfvén wave current tubes act like an 'external load' represented by a conductance $\Sigma_A \sim 1/\mu_0 V_A$ with V_A the Alfvén speed (a more accurate expression is given in the text in (10)). Therefore open field lines have a limited conductance.

TABLE 1. Characteristic Quantities for Satellite Interactions*

	Amalthea	Io	Europa	Ganymede	Callisto
Distance, R_J	2.54	5.9	9.4	15.0	26.3
Radius R, km	100†	1,820‡	1,565‡	2,640‡	2,420‡
u_0, km/s	4.9	56.8	104	177	322
n_e, cm^{-3}	20	1,500	10	1.5	0.1
B_0, nT	23,800	1,900	470	116	30
V_A, km/s	38,700	356	1,080	688	689
M_A	1.27×10^{-4}	0.16	0.10	0.26	0.47
θ_A, deg	0.007	9.1	5.7	14.6	25.0
$U = 2B_0u_0R$, kV	23.3	393	153	108	46.8
Σ_A, Ω^{-1}	0.021	2.2	0.74	1.2	1.2
I_{max}, A	926	1.74×10^6	233,000	246,000	98,000
m_{max}, A km	1.5×10^5	4.5×10^9	5.6×10^8	1.1×10^9	4.3×10^8
P_{max}, W	9×10^6	2.7×10^{11}	1.4×10^{10}	1.1×10^{10}	2.1×10^9
Σ_A/R, $(\Omega$ m$)^{-1}$	2.1×10^{-7}	1.2×10^{-6}	4.7×10^{-7}	4.5×10^{-7}	5×10^{-7}

*See text.
†Intermediate between long and short dimensions.
‡*B. A. Smith et al.* [1979].

4. A complex system of Alfvén current tubes is set up in this way which depends strongly on the plasma and magnetic field distribution and particularly also on reflecting boundaries like the Io-torus boundary and the Jovian ionosphere. The interaction between Io and the torus boundary or Jovian ionosphere occurs only if the round trip travel time of the Alfvén wave to the reflecting boundary and back is short enough for the returning wave to reach Io.

5. The Alfvén wave system may produce enhanced radiation belt particle diffusion in the Io-torus and plasma heating.

6. The interaction between Io and the Jovian ionosphere is strongest under conditions where the northern or southern magnetic pole of Jupiter's dipole tips toward Io with a strong preference for the northern emissions. This effect together with the beaming of the emissions is proposed to explain the maximum occurrence rate of decametric radio emissions around maximum northern latitudes.

Acknowledgments. This work was financially supported by the Bundesministerium fuer Forschung und Technologie (BMFT). Part of this work was completed while I was visiting the Laboratory for Extraterrestrial Physics of NASA Goddard Space Flight Center, the hospitality of which is greatly appreciated. Discussions on some aspects of this work with C. K. Goertz, D. Stern, M. Goldstein, M. Acuna, and J. Fejer are also gratefully acknowledged.

The Editor thanks C. K. Goertz and M. G. Kivelson for their assistance in evaluating this paper.

REFERENCES

Acuna, M. H., and N. F. Ness, Results from the GSFC fluxgate magnetometer on Pioneer 11, in *Jupiter*, edited by T. Gehrels, pp. 830–847, University of Arizona Press, Tucson, 1976.

Bridge, H. S., J. W. Belcher, A. J. Lazarus, J. D. Sullivan, R. McNutt, F. Bagenal, J. D. Scudder, E. C. Sittler, Jr., G. L. Siscoe, V. M. Vasyliunas, C. K. Goertz, and C. M. Yeates, Plasma observations near Jupiter: Initial results from Voyager 1, *Science, 203,* 47–50, 1979.

Broadfoot, A. L., J. S. Belton, B. R. Sandel, D. E. Schemansky, P. Z. Takacs, J. B. Holberg, J. M. Ajello, S. K. Atreya, T. M. Donahue, H. W. Moos, J. L. Bertaux, J. E. Blamont, D. F. Strobel, F. C. McConnell, A. Dalgarno, R. Goody, and M. B. McElroy, Extreme ultraviolet observations from Voyager 1 encounter with Jupiter, *Science, 203,* 39–41, 1979.

Cloutier, P. A., R. E. Daniell, Jr., A. J. Dessler, and T. W. Hill, A cometary ionosphere model for Io, *Astrophys. Space Sci., 55,* 93–112, 1978.

Dessler, A. J., and T. W. Hill, Jovian longitudinal control of Io-related radio emissions, *Astrophys. J., 226,* 664–675, 1979.

Drell, S. D., H. M. Foley, and M. A. Ruderman, Drag and propulsion of large satellites in the ionosphere: An Alfvén propulsion engine in space, *J. Geophys. Res., 70,* 3131–3146, 1965.

Dulk, G. A., Io-related radio emission from Jupiter, Ph.D. dissertation, Univ. of Colo., Boulder, 1965.

Goertz, C. K., Jupiter's ionosphere and magnetosphere, *Planet. Space Sci., 21,* 1389–1398, 1973.

Goertz, C. K., and P. A. Deift, Io's interaction with the magnetosphere, *Planet. Space Sci., 21,* 1399–1415, 1973.

Goldreich, P., and D. Lynden-Bell, Io, a Jovian unipolar inductor, *Astrophys. J., 156,* 59, 1969.

Gurnett, D. A., Sheath effects and related charged-particle acceleration by Jupiter's satellite Io, *Astrophys. J., 175,* 525–533, 1972.

Gurnett, D. A., R. R. Shaw, R. R. Anderson, W. S. Kurth, and F. L. Scarf, Whistlers observed by Voyager 1: Detection of lightning on Jupiter, submitted to *Geophys. Res. Lett.,* 1979.

Jeffrey, A., and T. Taniuti, *Non-linear Wave Propagation With Applications to Physics and Magnetohydrodynamics,* Academic, New York, 1964.

Kivelson, M. G., J. A. Slavin, and D. J. Southwood, Magnetospheres of Galilean satellites and their interaction with Jovian magnetosphere, *Science, 205,* 491–493, 1979.

Kumar, S., The stability of an SO_2 atmosphere on Io, *Nature, 280,* 758–760, 1979.

Mallinckrodt, A. J., and C. W. Carlson, Relations between transverse electric fields and field-aligned currents, *J. Geophys. Res., 83,* 1426–1432, 1978.

Maltsev, Y. P., W. B. Lyatsky, and A. M. Lyatskaya, Currents over the auroral arc, *Planet. Space Sci., 25,* 53, 1977.

McNutt, R. L., J. W. Belcher, J. D. Sullivan, F. Bagenal, and H. S. Bridge, Departure from rigid co-rotation of plasma in Jupiter's dayside magnetosphere, *Nature, 280,* 803, 1979.

Mekler, Y., and A. Eviatar, Thermal electron density in the Jovian magnetosphere, *J. Geophys. Res., 83,* 5679–5684, 1978.

Ness, N. F., M. H. Acuna, R. P. Lepping, L. F. Burlaga, K. W. Behannon, and F. M. Neubauer, Magnetic field studies at Jupiter by Voyager 1: Preliminary results, *Science, 203,* 42–46, 1979.

Neubauer, F. M., Possible strengths of dynamo magnetic fields of the Galilean satellites and of Titan, *Geophys. Res. Lett., 5,* 905–908, 1978.

Pearl, J., R. Hanel, V. Kunde, W. Maguire, K. Fox, S. Gupta, C. Ponnamperuma, and F. Raulin, Identification of gaseous SO_2 and new upper limits for other gases on Io, *Nature, 280,* 755–758, 1979.

Piddington, J. H., Jupiter's magnetosphere, *Rep. 67-63,* Univ. of Iowa, Iowa City, 1967.

Piddington, J. H., and J. F. Drake, Electrodynamic effects of Jupiter's satellite Io, *Nature, 217,* 935–937, 1968.

Shawhan, S. D., C. K. Goertz, R. F. Hubbard, D. A. Gurnett, and G. Foyce, Io-accelerated electrons and ions in *The Magnetospheres of the Earth and Jupiter,* edited by V. Formisano, D. Reidel, Hingham, Mass., 1975.

Smith, B. A., L. A. Soderblom, T. V. Johnson, A. P. Ingersoll, S. A. Collins, E. M. Shoemaker, G. E. Hunt, H. Masursky, M. H. Carr, M. E. Davies, A. F. Cook II, F. Boyce, G. E. Danielson, T. Owen, C. Sagan, R. F. Beebe, F. Veverka, R. G. Shom, J. F. McCauley, D. Morrison, G. A. Briggs, and V. E. Suomi, The Jupiter system through the eyes of Voyager 1, *Science, 203,* 13–31, 1979.

Smith, R. A., Models of Jovian decametric radiation, in *Jupiter,* edited by T. Gehrels, pp. 1146–1189, University of Arizona Press, Tucson, 1976.

Warwick, J. W., J. B. Pearce, A. C. Riddle, J. K. Alexander, M. D. Desch, M. L. Kaiser, J. R. Thieman, T. D. Carr, S. Gulkis, A. Boischot, C. C. Harvey, and B. M. Pederson, Voyager 1 planetary radio astronomy observations near Jupiter, *Science, 203,* 55–57, 1979.

(Received July 25, 1979;
revised October 24, 1979;
accepted November 1, 1979.)